Atomic shell structure from the Single-Exponential Decay Detector

De Silva, Piotr; Korchowiec, Jacek; Wesolowski, Tomasz Adam

How to cite

DE SILVA, Piotr, KORCHOWIEC, Jacek, WESOLOWSKI, Tomasz Adam. Atomic shell structure from the Single-Exponential Decay Detector. In: The Journal of chemical physics, 2014, vol. 140, n° 16, p. 164301. doi: 10.1063/1.4871501

This publication URL: https://archive-ouverte.unige.ch/unige:39941
Publication DOI: 10.1063/1.4871501

Atomic shell structure from the Single-Exponential Decay Detector

Piotr de Silva,[1,2,a] Jacek Korchowiec,[1] and Tomasz A. Wesolowski[2]
[1]*K. Gumiński Department of Theoretical Chemistry, Faculty of Chemistry, Jagiellonian University, R. Ingardena 3, 30-060 Kraków, Poland*
[2]*Département de Chimie Physique, Université de Genève, 30, quai Ernest-Ansermet, CH-1211 Genève 4, Switzerland*

(Received 4 March 2014; accepted 4 April 2014; published online 22 April 2014)

The density of atomic systems is analysed via the Single-Exponential Decay Detector (SEDD). SEDD is a scalar field designed to explore mathematical, rather than physical, properties of electron density. Nevertheless, it has been shown that SEDD can serve as a descriptor of bonding patterns in molecules as well as an indicator of atomic shells [P. de Silva, J. Korchowiec, and T. A. Wesolowski, ChemPhysChem **13**, 3462 (2012)]. In this work, a more detailed analysis of atomic shells is done for atoms in the Li–Xe series. Shell populations based on SEDD agree with the Aufbau principle even better than those obtained from the Electron Localization Function, which is a popular indicator of electron localization. A link between SEDD and the local wave vector is given, which provides a physical interpretation of SEDD. © *2014 AIP Publishing LLC*. [http://dx.doi.org/10.1063/1.4871501]

I. INTRODUCTION

The concept of electrons occupying shells in atoms is fundamental for our understanding of the electronic structure of atomic and molecular systems. This idea is based on the solutions of the Schrödinger equation for the hydrogen atom, for which degenerate orbitals forming each shell share the same principal quantum number. This one-electron picture can be extended to many-electron atoms, where the degeneracy of subshells is lifted. The Aufbau principle states that electrons successively fill the available one-electron levels, which gives rise to the concept of electronic configuration. This is the main idea behind the Hartree-Fock method, which is the cornerstone of quantum chemistry.

In terms of atomic orbitals, the notion of a shell is quite clear. It is simply a set of orbitals with the same principal quantum number. However, many attempts have been made to relate this concept to the total electron density.[1–16] Since orbital densities overlap each other, the concept of atomic shells in real space is somehow lost.[17,18] It is conjectured, although never proved, that the electron density of atoms is a monotonically decaying function.[19,20] Therefore, it does not exhibit any shell structure itself. Different transformations of the density or the approximate many-electron wavefunction have led to descriptors that succeeded in resolving the shell structure of atoms. Conceptually, the simplest approach is to investigate radial densities,[1,4] which exhibit maxima corresponding to different shells. Other descriptors based on electron density include Laplacian of the density,[5,6] reduced density gradient,[7] one-electron potential,[8] electron inhomogeneity measure,[9] and local wave number.[10–12] Some of the developed descriptors take a direct input from orbitals or one-particle density matrix. These are, for example, the electronic stress tensor[13,14] or the Electron Localization Function (ELF).[15,16] All these functions reveal, to some extent at least, atomic shells. Usually, the boundaries between them are indicated by some characteristic points of the descriptor, like stationary or inflection points. This enables to define atomic radii and integrate the density over the corresponding regions to obtain shell populations. These depend significantly on the descriptor used, however, usually they give electron numbers approximately matching those predicted by the Aufbau principle.

In the present work, we verify the ability of the Single Exponential Decay Detector (SEDD) to resolve the shell structure of atoms. SEDD was introduced as a tool for analysis of bonding patterns of molecular systems.[21] It was shown that bonding patterns revealed by SEDD agree with chemical intuition and exhibit essentially the same features as ELF. It was also shown that delocalized domains of SEDD provide a fingerprint of aromaticity in flat carbon rings.[22] The main feature of SEDD is that it depends only on the electron density and its first and second derivatives. No orbitals are needed in its evaluation, what makes it a well defined quantity at any level of theory. The range of significant values of SEDD turns out to be practically system-independent, what facilitates visualization and comparison of the results between different systems. In the present work, we show that the analysis of SEDD allows to identify in real space all the expected atomic shells for all the atoms from lithium to xenon. Moreover, it divides the space into regions dominated by a single shell as well as high-overlap regions. Maxima of SEDD in the overlap region define shell radii. Integration of the density over resulting shells yields electron numbers, which approximately agree with the expected ones.

The usefulness of SEDD as a tool for visualization of bonding patterns demonstrated in our previous works[21,22] calls for a physical interpretation of the quantity $\xi(\mathbf{r}) = [\frac{1}{\rho(\mathbf{r})}(\nabla(\frac{\nabla\rho(\mathbf{r})}{\rho(\mathbf{r})})^2)]^2$ that SEDD visualizes. To this end, the discussion of mathematical features of SEDD for atomic and

[a]Author to whom correspondence should be addressed. Electronic mail: piotr.desilva@unige.ch

molecular densities is supplemented in this work by the formal analysis of the link between SEDD and the local wave number.[10–12] As SEDD is a dimensionless quantity, we show that this is achieved by making a reference to the homogeneous electron gas (HEG) model.

II. SINGLE-EXPONENTIAL DECAY DETECTOR

A. Built-in properties of $\xi(\mathbf{r})$ for atomic and molecular densities

The Single-Exponential Decay Detector was introduced as an orbital-free descriptor of bonding patterns in molecular systems. The idea behind was to reveal regions of space, where the electron density decays exponentially from an arbitrary point in space, i.e., $\rho(\mathbf{r}) \sim e^{-\lambda|\mathbf{r}-\mathbf{r_0}|}$. In order to visualize such regions, the following dimensionless scalar field was constructed:

$$\xi(\mathbf{r}) = \left(\frac{\nabla \left(\frac{\nabla\rho(\mathbf{r})}{\rho(\mathbf{r})} \right)^2}{\rho(\mathbf{r})} \right)^2 . \tag{1}$$

Inserting $\rho(\mathbf{r}) \sim e^{-\lambda|\mathbf{r}-\mathbf{r_0}|}$ into Eq. (1) gives $\xi(\mathbf{r}) = 0$, therefore, $\xi(\mathbf{r})$ detects regions of single-exponential electron density.

For molecular systems, there are two limiting cases, where the density is known to be of exponential form. One is the behaviour at nuclei, where the exponent is determined by nuclear charge $\rho(\mathbf{r}) \sim e^{-2Z_\alpha|\mathbf{r}-\mathbf{r}_\alpha|}$. This is reflected by the Kato cusp condition[23]

$$\frac{\partial}{\partial r_\alpha}\rho_{av}(r_\alpha)\Big|_{r_\alpha=0} = -2Z_\alpha\rho(0), \tag{2}$$

where $\rho_{av}(r_\alpha)$ is the spherically averaged density, Z_α is the nuclear charge, and r_α is a vector originating at the nucleus. The second asymptotic limit is given for large distances from the molecule, where the decay of the density if determined by the ionization potential (I): $\rho(\mathbf{r}) \sim e^{-2\sqrt{2I}|\mathbf{r}|}$.[24]

Based on these results, it is expected that $\xi(\mathbf{r})$ will approach 0 near nuclei. This is in agreement with the fact that this region is occupied by 1s electrons of a given atom and not much penetrated by those from higher shells. The same behaviour could also be expected far from the molecule, however, this time both numerator and denominator in Eq. (1) tend to 0. In fact, ρ^2 decays faster than $(\nabla(\frac{\nabla\rho}{\rho})^2)^2$ and $\xi(\mathbf{r}) \to +\infty$.

Density in bonding regions is largely determined by the overlap of atomic densities and as such is not expected to behave exponentially (even piecewise). However, such density is characterized by small density gradients. In particular, at the bond critical point (BCP) $\nabla\rho(\mathbf{r}) = 0$. Therefore, the density at BCP can be formally treated as single-exponential up to the first order with $\lambda = 0$ and $\xi(\mathbf{r}) = 0$. Finally, $\xi(\mathbf{r})$ is equal to 0 at stationary points of $(\frac{\nabla\rho}{\rho})^2$, although, the density at these points is not locally exponential.

In a chemically intuitive description of molecular electronic structure, electrons are localized in core atomic shells, bonds, or lone pairs. Properties of $\xi(\mathbf{r})$ suggest that it may be useful in visualization of bonding patterns understood as a distribution of localized electron pairs. Although $\xi(\mathbf{r})$ was designed to discover single-exponential densities, it turned out that it provides rich information about the chemical structure of molecules.

Summarizing, $\xi(\mathbf{r})$ is expected to have low values near nuclei, around bond critical points, and possibly in some other regions. Conversely, far from the molecule $\xi(\mathbf{r})$ exhibits an exponential explosion. This rapid behaviour is problematic from the point of view of visualization, as the informative range of values becomes very large. To circumvent this undesired feature, a logarithmic transformation was introduced to flatten the scale. This leads to the following definition of SEDD, which was introduced in Ref. 21

$$SEDD^*(\mathbf{r}) = \ln\xi(\mathbf{r}) = \ln\left[\left(\frac{\nabla \left(\frac{\nabla\rho(\mathbf{r})}{\rho(\mathbf{r})} \right)^2}{\rho(\mathbf{r})} \right)^2 \right]. \tag{3}$$

The range of values of $SEDD^*(\mathbf{r})$ is $[-\infty, \infty]$, and negative values appear where $\xi(\mathbf{r}) < 1$. Nevertheless, all the essential information provided by SEDD are contained solely in $\xi(\mathbf{r})$ and the logarithmic transformation is applied only for the convenience of visualization. Scalar fields are typically visualized as two-dimensional maps or three-dimensional isosurfaces, therefore, establishing the meaningful range of values is important. In previous papers, we have shown that plotting 2D maps of SEDD in the range from 2 to 15 is enough to capture all its features,[21] whereas for 3D surfaces, $SEDD^*(r) = 5.0$ is a convenient choice for the isovalue.[22] Here, we notice that the choice of the transformation letting SEDD have negative values was not very fortunate. In particular, because it leads to singularities wherever $\xi(\mathbf{r}) = 0$, which is inconvenient for plotting SEDD in one dimension. To amend this problem, we redefine the transformation by shifting $\xi(\mathbf{r})$ by 1

$$SEDD(\mathbf{r}) = \ln(1+\xi(\mathbf{r})) = \ln\left[1 + \left(\frac{\nabla \left(\frac{\nabla\rho(\mathbf{r})}{\rho(\mathbf{r})} \right)^2}{\rho(\mathbf{r})} \right)^2 \right]. \tag{4}$$

This minor modification with respect to the definition in Eq. (3) does not alter the recommended isovalues as the only significant differences between $SEDD(\mathbf{r})$ and $SEDD^*(\mathbf{r})$ appear for very low values of $\xi(\mathbf{r})$, which lie below the range of SEDD recommended for graphical representation of bonding patterns.[21,22]

Contrary to some other bonding descriptors, the formula of SEDD was not explicitly derived to reveal localized electrons. It was designed as a dimensionless scalar field showing some particular geometric features of electron density. Nevertheless, its relation to localization is apparent due to the ability of SEDD to reveal expected qualitative features of bonding in molecules.

B. Relation with the local wave vector

The main idea behind SEDD is that the ratio $(\frac{\nabla\rho(\mathbf{r})}{\rho(\mathbf{r})})^2$ is constant for locally single-exponential densities. The quantity $\frac{\nabla\rho(\mathbf{r})}{\rho(\mathbf{r})}$ is known in the literature as the local wave vector

$\mathbf{k}(\mathbf{r}) = \frac{\nabla\rho(\mathbf{r})}{\rho(\mathbf{r})}$,[11] which is closely related to the local momentum $\mathbf{p}(\mathbf{r}) = -\frac{\hbar}{2}\mathbf{k}(\mathbf{r})$.[12] The theory of local representation of operators[12,25] has been used by Bohórquez *et al.*,[12,26,27] who have derived a density-dependent detector of localized electrons based on the local momentum. Square of the local wave vector is also proportional to one of the terms in the functional derivative of the von Weizsäcker kinetic energy functional

$$v_t^W[\rho](\mathbf{r}) = \frac{\delta T_w[\rho(\mathbf{r})]}{\delta\rho(\mathbf{r})} = \frac{1}{8}\frac{|\nabla\rho(\mathbf{r})|^2}{\rho(\mathbf{r})^2} - \frac{1}{4}\frac{\nabla^2\rho(\mathbf{r})}{\rho(\mathbf{r})}. \quad (5)$$

The potential $v_t^W[\rho](\mathbf{r})$ can also be interpreted as the local representation of the kinetic energy operator. This suggests that SEDD can be viewed not only as a purely mathematical field detecting geometrical features of the density, but also a more physical meaning can be attributed. The behaviour of the local wave number $k(\mathbf{r}) = |\mathbf{k}(\mathbf{r})|$ is known[10,12] to reflect shells in atoms. In principle, shells correspond to plateaus of $k(\mathbf{r})$. Below, we present $\xi(\mathbf{r})$ as a dimensionless quantity to detect such plateaus. Dimensionlessness is a desired feature for a bonding descriptors to remain universal. In general, it can be achieved by dividing the analysed quantity by its counterpart from some reference model system. Below $\xi(\mathbf{r})$ is presented a dimensionless quantity obtained using a particular reference – the homogeneous electron gas.

It is known that the density of atomic systems is approximately piecewise exponential.[28] This means that the local wave number $k(\mathbf{r})$ should consist of local plateaus, each adopting a different value and corresponding to a different shell. Kohout *et al.*[10] have shown that this is essentially true for valence shells, while for the inner ones $k(\mathbf{r})$ is strongly curved, reflecting the fact that shells interpenetrate each other. Nevertheless, the model of shells exhibiting different local momenta still holds to large extent. The boundaries can be defined by inflection points of $k(r)$, which leads to a reasonably good agreement between resulting electron populations and the Aufbau principle.[12]

The analysis of the electronic structure of atomic and molecular systems is often done in terms of dimensionless scalar fields. One of such dimensionless quantities is, well known in Density Functional Theory, the reduced density gradient[29]

$$s(\mathbf{r}) = \frac{|\nabla\rho(\mathbf{r})|}{2k_F\rho(\mathbf{r})} = \frac{|\nabla\rho(\mathbf{r})|}{2(3\pi^2)^{1/3}\rho^{4/3}(\mathbf{r})}, \quad (6)$$

where k_F is the Fermi wave vector. The analysis of $s(\mathbf{r})$ has shown that it reveals the shell structure of atoms.[7] It has also been used in the definition of the Non-Covalent Interactions (NCI) index for the analysis of non-covalent interactions.[30] Combining the definition of $s(\mathbf{r})$ (Eq. (6)) and $k(\mathbf{r})$ immediately leads to an interpretation of the reduced density gradient as a dimensionless local wave number, where $k(\mathbf{r})$ is divided by the diameter of the Fermi sphere in the HEG model,

$$s(\mathbf{r}) = \frac{k(\mathbf{r})}{2k_F}. \quad (7)$$

Since the regions where the density is dominated by a single atomic shell should be characterized by plateaus of $k(\mathbf{r})$, the magnitude of its gradient $|\nabla k(\mathbf{r})|$ provides a measure of localization of a given shell. The same applies to the quantity $(\nabla\mathbf{k}^2(\mathbf{r}))^2$, where absolute values of vector fields are replaced by its squares. Square of the local wave vector, in turn, can be viewed as the local representation of the single-particle kinetic energy. In order to obtain a dimensionless field, $(\nabla\mathbf{k}^2(\mathbf{r}))^2$ has to be divided by another quantity of the same dimension. Similarly as for the reduced density gradient, the homogeneous electron gas could be used as a reference system (Eq. (7)). However, the analogous quantity $(\nabla k_F^2)^2$ is not necessarily a good choice, as for HEG it would be equal to 0. Instead, a suitable power of k_F itself can be used as a reference, leading to a dimensionless field in the following form:

$$\eta(\mathbf{r}) = \left(\frac{\nabla\mathbf{k}^2(\mathbf{r})}{k_F^3}\right)^2. \quad (8)$$

Replacing $\mathbf{k}(\mathbf{r})$ and k_F by their explicit dependence on the density, leads to a quantity that is proportional to $\xi(\mathbf{r})$ (Eq. (1))

$$\xi(\mathbf{r}) = (3\pi^2)^2\eta(\mathbf{r}). \quad (9)$$

This argument gives another interpretation to SEDD in terms of physically motivated quantities. According to it, for localized electrons, the gradient of the local kinetic energy

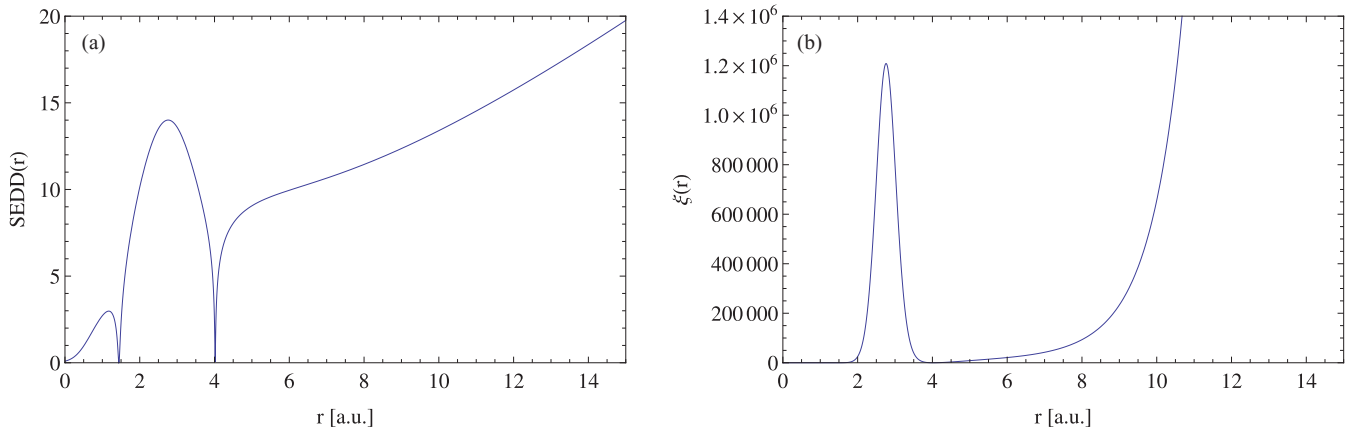

FIG. 1. *SEDD*(r) (a) and $\xi(r)$ (b) calculated for the $1s^2 2s^2$ configuration of an artificial system of four non-interacting electrons in $-1/r$ potential.

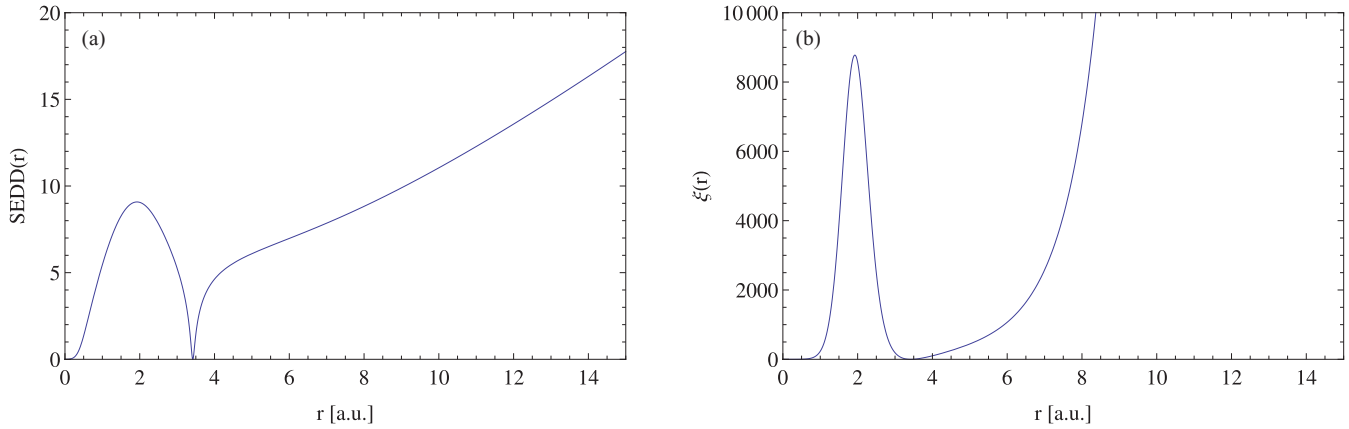

FIG. 2. *SEDD*(*r*) (a) and $\xi(r)$ (b) calculated for the $1s^2 2s^2 2p_x^{(2/3)} 2p_y^{(2/3)} 2p_z^{(2/3)}$ configuration of an artificial system of six non-interacting electrons in $-1/r$ potential.

is small compared to the volume of the corresponding Fermi sphere.

III. RESULTS

A. Shells in an artificial analytical system: non-interacting electrons in $-1/r$ potential

Before analysing more realistic atomic densities obtained with the Hartree-Fock method using the Linear Combination of Atomic Orbitals (LCAO) approximation (Sec. III B), we focus on an artificial, non-physical example. This auxiliary analysis is done to better understand the link between the structure of individual atomic orbitals and the shell structure indicated by SEDD. The simplest model for an atom is the system of non-interacting electrons moving in a central $-1/r$ potential. The wavefunction of such system is a single Slater determinant composed of hydrogen orbitals occupied by a given number of electrons (assuming lack of degeneracy). Such model is suitable to verify the applicability of SEDD in resolving the shell structure in real space. Although hydrogen orbitals with the same principal quantum number are degenerate, in this model, we occupy orbitals with lower azimuthal quantum number first. This is done to mimic the Aufbau principle for interacting many-electron atoms, for which this degeneracy is lifted.

For the one- or two-electron system in its ground state, the situation is very simple. Only the lowest-lying $1s$ orbital is occupied and the density is exactly of the single-exponential form (atomic units are used throughout this work)

$$\rho(r,\theta,\phi) = |\varphi_{1s}(r,\theta,\phi)|^2 = \frac{1}{\pi} e^{-2r}, \tag{10}$$

therefore, $SEDD(r) = 0$. The next two electrons added occupy the $2s$ orbital. This leads to a more complex shape of SEDD (Fig. 1(a)). Close to the nucleus SEDD is close to 0 and then increases while moving outwards. It drops to 0 at 1.44 bohrs due to the presence of a stationary point in $\frac{|\nabla\rho(r)|}{\rho(r)}$, then rises again to reach the maximum at 2.76 bohrs. SEDD has another sharp minimum at 4.02 bohrs, after passing which, it continues increasing due to the reason discussed in Sec. II. The second maximum at $r_b = 2.76$ bohrs divides the density into two shells. Due to the logarithmic transformation in the definition of SEDD (Eq. (4)), the differences between values for localized and overlapping regions are not that evident at first glance. Plotting $\xi(r)$ (Eq. (1)) instead leaves no doubt, where the boundary between shells lies (Fig. 1(b)). Integrating the density within the sphere of 2.76 bohrs radius, gives

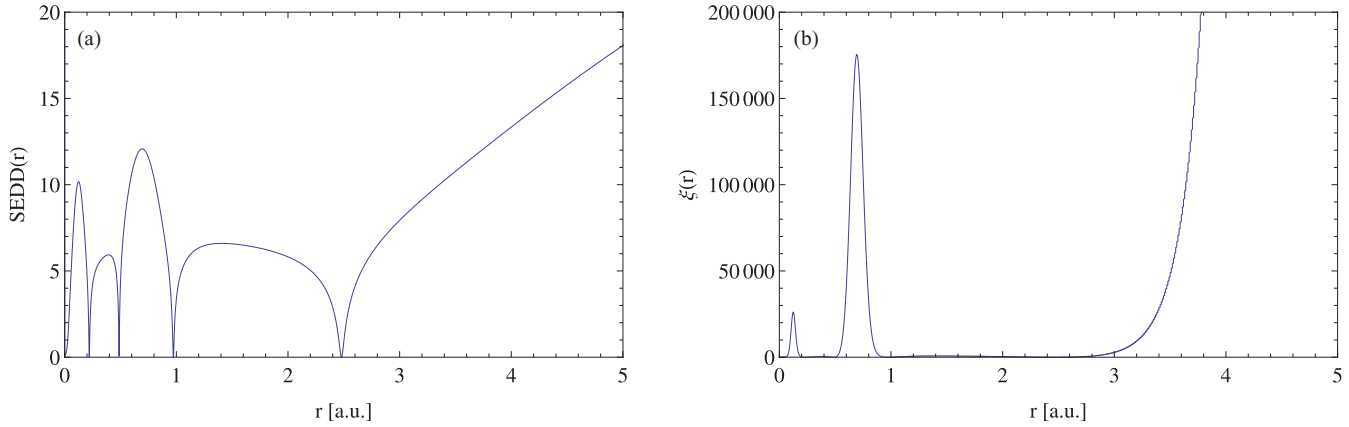

FIG. 3. *SEDD*(*r*) (a) and $\xi(r)$ (b) for the argon atom.

TABLE I. Electron populations and radii (a.u.) of shells represented by SEDD.

Atom	P_K	r_K	P_L	r_L	P_M	r_M	P_N	r_N	P_O
Li (^{2}S)	2.00	1.514	1.00						
Be (^{1}S)	1.98	0.951	2.02						
B (^{2}P)	1.98	0.695	3.02						
C (^{3}P)	1.99	0.536	4.01						
N (^{4}S)	1.99	0.429	5.01						
O (^{3}P)	1.99	0.358	6.01						
F (^{2}P)	1.99	0.305	7.01						
Ne (^{1}S)	1.98	0.264	8.02						
Na (^{2}S)	1.97	0.232	8.05	2.175	0.98				
Mg (^{1}S)	1.96	0.207	8.03	1.615	2.01				
Al (^{2}P)	1.95	0.187	8.01	1.334	3.02				
Si (^{3}P)	1.95	0.170	8.00	1.131	4.05				
P (^{4}S)	1.94	0.156	7.98	0.976	5.08				
S (^{3}P)	1.94	0.144	7.97	0.862	6.10				
Cl (^{2}P)	1.93	0.134	7.95	0.770	7.11				
Ar (^{1}S)	1.93	0.125	7.94	0.694	8.13				
K (^{2}S)	1.93	0.117	7.93	0.632	8.18	3.158	0.94		
Ca (^{1}S)	1.92	0.110	7.92	0.580	8.17	2.457	1.98		
Sc (^{2}D)	1.92	0.104	7.92	0.538	8.64	2.197	2.50		
Ti (^{3}F)	1.91	0.098	7.95	0.501	9.58	2.100	2.56		
V (^{4}F)	1.90	0.093	7.97	0.468	10.65	2.062	2.48		
Cr (^{7}S)	1.91	0.089	8.01	0.440	12.72	2.395	1.36		
Mn (^{6}S)	1.91	0.085	8.02	0.413	12.86	2.036	2.21		
Fe (^{5}D)	1.90	0.081	8.05	0.390	13.48	1.882	2.58		
Co (^{4}F)	1.90	0.078	8.06	0.369	14.49	1.841	2.55		
Ni (^{3}F)	1.90	0.075	8.09	0.351	15.61	1.847	2.39		
Cu (^{2}S)	1.90	0.072	8.13	0.334	18.01	2.506	0.96		
Zn (^{1}S)	1.89	0.069	8.16	0.318	17.78	1.826	2.17		
Ga (^{2}P)	1.90	0.067	8.16	0.303	17.85	1.621	3.08		
Ge (^{3}P)	1.88	0.064	8.20	0.290	17.76	1.421	4.16		
As (^{4}S)	1.88	0.062	8.19	0.277	17.66	1.263	5.27		
Se (^{3}P)	1.88	0.060	8.21	0.266	17.61	1.154	6.29		
Br (^{2}P)	1.88	0.058	8.21	0.255	17.57	1.061	7.34		
Kr (^{1}S)	1.87	0.056	8.25	0.246	17.48	0.981	8.39		
Rb (^{2}S)	1.89	0.055	8.21	0.236	17.47	0.916	8.48	3.592	0.91
Sr (^{1}S)	1.88	0.053	8.24	0.228	17.42	0.860	8.48	2.861	1.96
Y (^{2}D)	1.86	0.051	8.27	0.220	17.42	0.814	8.86	2.574	2.58
Zr (^{3}F)	1.87	0.050	8.28	0.213	17.41	0.774	9.67	2.452	2.77
Nb (^{6}D)	1.89	0.049	8.27	0.206	17.42	0.738	11.50	2.650	1.92
Mo (^{7}S)	1.85	0.047	8.33	0.200	17.40	0.704	13.17	2.992	1.25
Tc (^{6}S)	1.86	0.046	8.33	0.194	17.37	0.671	13.30	2.560	2.13
Ru (^{5}F)	1.87	0.045	8.32	0.188	17.39	0.643	15.36	3.146	1.06
Rh (^{4}F)	1.87	0.044	8.35	0.183	17.37	0.617	16.72	3.485	0.69
Pd (^{1}S)	1.87	0.043	8.37	0.178	17.35	0.592	18.41		
Ag (^{2}S)	1.87	0.042	8.37	0.173	17.35	0.569	18.82	3.465	0.58
Cd (^{1}S)	1.87	0.041	8.36	0.168	17.36	0.547	18.63	2.456	1.78
In (^{2}P)	1.86	0.040	8.40	0.164	17.31	0.526	18.56	2.122	2.86
Sn (^{3}P)	1.85	0.039	8.42	0.160	17.28	0.507	18.41	1.860	4.03
Sb (^{4}S)	1.84	0.038	8.44	0.156	17.28	0.490	18.25	1.668	5.19
Te (^{3}P)	1.83	0.037	8.45	0.152	17.26	0.473	18.19	1.537	6.27
I (^{2}P)	1.88	0.037	8.45	0.149	17.22	0.458	18.09	1.424	7.36
Xe (^{1}S)	1.86	0.036	8.44	0.145	17.23	0.443	18.02	1.328	8.46

1.95 electrons, which is very close to the exact occupation of the 1*s* shell.

In a six electron system, two electrons occupy the 2*p* subshell. We stress at this point that this is not a model for the carbon atom as electrons are non-interacting and the external potential is $-1/r$. As there are three degenerate 2*p* orbitals available, the exact wavefunction is not just a single Slater determinant. However, in this case the one-electron picture can be maintained at the cost of introducing fractional occupancies. Assuming that each of the 2*p* orbitals is occupied by 2/3 of the electron leads to the proper spherically symmetric density. Fig. 2(a) shows SEDD for such fictitious atom

TABLE II. Electron populations and radii (a.u.) of shells represented by ELF.

Atom	P_K	r_K	P_L	r_L	P_M	r_M	P_N	r_N	P_O
Li (^{2}S)	2.00	1.530	1.00						
Be (^{1}S)	2.02	1.021	1.98						
B (^{2}P)	2.03	0.752	2.96						
C (^{3}P)	2.07	0.585	3.93						
N (^{4}S)	2.10	0.472	4.90						
O (^{3}P)	2.12	0.398	5.88						
F (^{2}P)	2.14	0.343	6.86						
Ne (^{1}S)	2.16	0.298	7.84						
Na (^{2}S)	2.17	0.264	7.83	2.136	0.99				
Mg (^{1}S)	2.18	0.236	7.87	1.688	1.95				
Al (^{2}P)	2.19	0.214	7.86	1.398	2.94				
Si (^{3}P)	2.19	0.195	7.86	1.187	3.95				
P (^{4}S)	2.19	0.179	7.85	1.023	4.96				
S (^{3}P)	2.20	0.166	7.85	0.910	5.95				
Cl (^{2}P)	2.20	0.154	7.87	0.817	6.93				
Ar (^{1}S)	2.21	0.144	7.87	0.738	7.92				
K (^{2}S)	2.21	0.135	7.87	0.672	7.93	3.088	0.97		
Ca (^{1}S)	2.21	0.127	7.86	0.617	8.01	2.544	1.91		
Sc (^{2}D)	2.21	0.120	7.88	0.572	8.51	2.287	2.39		
Ti (^{3}F)	2.22	0.114	7.91	0.534	9.43	2.185	2.43		
V (^{4}F)	2.21	0.108	7.96	0.500	10.46	2.132	2.37		
Cr (^{7}S)	2.21	0.103	8.04	0.471	12.36	2.375	1.39		
Mn (^{6}S)	2.23	0.099	8.06	0.443	12.54	2.063	2.17		
Fe (^{5}D)	2.21	0.094	8.12	0.419	13.17	1.927	2.49		
Co (^{4}F)	2.23	0.091	8.16	0.398	14.12	1.873	2.48		
Ni (^{3}F)	2.22	0.087	8.22	0.378	15.17	1.849	2.38		
Cu (^{2}S)	2.23	0.084	8.29	0.361	17.17	2.151	1.30		
Zn (^{1}S)	2.24	0.081	8.33	0.344	17.21	1.799	2.23		
Ga (^{2}P)	2.23	0.078	8.38	0.329	17.26	1.610	3.11		
Ge (^{3}P)	2.22	0.075	8.42	0.314	17.23	1.430	4.13		
As (^{4}S)	2.24	0.073	8.44	0.301	17.12	1.277	5.20		
Se (^{3}P)	2.22	0.070	8.49	0.289	17.13	1.181	6.16		
Br (^{2}P)	2.23	0.068	8.49	0.277	17.14	1.095	7.14		
Kr (^{1}S)	2.23	0.066	8.53	0.267	17.10	1.017	8.14		
Rb (^{2}S)	2.23	0.064	8.54	0.257	17.07	0.950	8.17	3.500	0.95
Sr (^{1}S)	2.23	0.062	8.57	0.248	17.04	0.893	8.26	2.951	1.88
Y (^{2}D)	2.22	0.060	8.59	0.239	17.04	0.845	8.67	2.666	2.46
Zr (^{3}F)	2.25	0.059	8.58	0.231	17.06	0.805	9.49	2.545	2.62
Nb (^{6}D)	2.23	0.057	8.64	0.224	17.07	0.770	11.23	2.712	1.82
Mo (^{7}S)	2.25	0.056	8.64	0.217	17.07	0.735	12.76	2.974	1.27
Tc (^{6}S)	2.23	0.054	8.67	0.210	17.08	0.701	12.82	2.512	2.21
Ru (^{5}F)	2.24	0.053	8.68	0.204	17.10	0.674	14.77	2.985	1.21
Rh (^{4}F)	2.26	0.052	8.68	0.198	17.11	0.647	16.95		
Pd (^{1}S)	2.22	0.050	8.77	0.193	17.09	0.622	17.92		
Ag (^{2}S)	2.23	0.049	8.79	0.188	17.08	0.598	17.82	2.749	1.08
Cd (^{1}S)	2.23	0.048	8.80	0.183	17.07	0.575	17.90	2.331	1.99
In (^{2}P)	2.24	0.047	8.80	0.178	17.08	0.554	17.90	2.076	2.96
Sn (^{3}P)	2.24	0.046	8.85	0.174	17.04	0.534	17.79	1.846	4.08
Sb (^{4}S)	2.24	0.045	8.83	0.169	17.06	0.515	17.66	1.662	5.22
Te (^{3}P)	2.23	0.044	8.85	0.165	17.05	0.498	17.69	1.555	6.17
I (^{2}P)	2.23	0.043	8.87	0.161	17.05	0.482	17.68	1.455	7.17
Xe (^{1}S)	2.22	0.042	8.87	0.157	17.07	0.467	17.63	1.362	8.21

comprising six non-interacting electrons. SEDD has a maximum at $r_b = 1.93$ bohrs, which constitutes the border between the first and the second shell. Again, the plot of $\xi(r)$ (Fig. 2(b)) is more straightforward in depicting the boundary. The integration of the density within such defined shell gives 1.86 electrons. Compared to the four electron case, the deviation from the expected number of electrons in the first shell is slightly larger. Upon adding two $2p$ electrons, the maximum of SEDD moved inwards as expected, however, too much to yield the same number of electrons. Also another maximum of SEDD, lying within the first shell of the four electron system, is not present in this case. The value of SEDD at the

maximum dividing the shells is smaller by 5, which translates to two orders of magnitude difference for $\xi(r)$.

B. Shells in realistic atoms

The example of model systems shows that SEDD is able to distinguish atomic shells. The integration of the density within them, gives numbers of electrons that agree approximately with the Aufbau principle. Verifying the performance of SEDD in resolving atomic shells in a more realistic model of atoms is the next step. In our previous work,[21] we have shown that SEDD qualitatively distinguishes five shells of the xenon atom calculated at the Kohn-Sham level. In this work, we have calculated spherically averaged electron densities of atoms throughout the periodic table from lithium to xenon. The densities were obtained from Hartree-Fock wavefunctions calculated with ADF program[31] using the QZ4P Slater-type basis set.

As an example, $SEDD(r)$ and $\xi(r)$ for the argon atom have been plotted in Fig. 3. SEDD distinguishes five regions, separated by points where $SEDD(r) = 0$. The first four regions exhibit a maximum of SEDD, while in the most outer one SEDD goes monotonically to infinity. Since argon has only three shells, it is clear that only two of four maxima can represent shell boundaries. These are the ones with the highest SEDD values, while the remaining two lie within the second and the third atomic shell. This structure means that SEDD reveals regions dominated by a single shell, as well as regions of significant overlap between two neighbouring shells. The latter ones have significantly higher SEDD values and respective maxima represent shell boundaries. This is more apparent from the plot of $\xi(r)$, where the only pronounced features are two sharp maxima and the explosion in the asymptotic region. The maxima in regions dominated by a single shell have lower values and result from still imperfect localization of these shells. The points where $SEDD(r) = 0$ can be interpreted as boundaries between these two kinds of regions and they appear where $\frac{\nabla\rho(r)}{\rho(r)}$ has a stationary point.

For other atoms, the same features are present and the expected number of atomic shells can be discerned. Integration of the density over the shells gives their populations. The location of SEDD maxima indicating shell boundaries and respective electron populations are summarized in Table I. For the second row of the periodic table, shell populations are nearly perfect. While moving towards higher atomic numbers, the population of the first shell decreases, reaching 1.86 electrons for xenon. Populations of the second shell are overestimated in most of the cases and the deviation increases with the size of the atom. For the remaining shells, the deviations from the expected numbers can reach 0.8 electrons. As the magnitude of deviations increases abruptly for scandium, it seems that *d* electrons are not likely to localize too much in the real space.

Different methods have been proposed to resolve atomic shells in real space and obtain corresponding populations by integration of the density. Perhaps, the most well known method is ELF, therefore, it is useful to compare the performance of SEDD with it. Direct comparison with results reported in literature[16] could be affected by different wavefunctions used in calculations. For this reason, we have also calculated ELF from the same orbitals which had been used in SEDD calculations. We have calculated ELF with DGrid program,[32] using the following spin-resolved formula:

$$ELF = \left[1 + \left(\frac{\tau - \frac{1}{8}\frac{(\nabla\rho_\alpha)^2}{\rho_\alpha} - \frac{1}{8}\frac{(\nabla\rho_\beta)^2}{\rho_\beta}}{2^{2/3}c_F\left(\rho_\alpha^{5/3} + \rho_\beta^{5/3}\right)}\right)^2\right]^{-1}, \qquad (11)$$

where τ is kinetic energy density and $\rho_{\alpha,\beta}$ are spin densities.

The shell boundaries given by maxima of ELF and corresponding electron populations are given in Table II. General pictures given by SEDD and ELF are rather similar. The most apparent difference is the behaviour of the population in the first shell, which increases with the atomic number for ELF.

The overall performance in discerning atomic shells can be characterized in terms of maximum and average deviations from ideal shell populations. Table III summarizes these numbers for SEDD and ELF. For both descriptors, discrepancies tend to larger values for more outer shells. For every shell, SEDD performs better than ELF with respect to the maximum deviation. In terms of the average discrepancy, SEDD is better for the first three shell, ELF is better for the fourth one, and both descriptors are comparable for the fifth shell. The deviation averaged over all shells for SEDD is noticeably smaller than for ELF. It has to be stressed that SEDD depends solely on the total electron density, while ELF is directly dependent on orbitals, therefore, this result is rather unexpected.

TABLE III. Deviations of shell populations, obtained by integration of the density, from ideal shell populations.

	SEDD		ELF	
Shell	max	Average	max	Average
K	0.17	0.09	0.26	0.20
L	0.45	0.17	0.87	0.37
M	0.78	0.41	0.96	0.66
N	0.82	0.34	0.95	0.27
O	0.92	0.29	1.00	0.28
All	0.92	0.24	1.00	0.37

IV. CONCLUSIONS

In our previous works, the SEDD was proposed as an arbitrary gauge of the character of the local decay of electron density in molecular systems. In this work, we have shown that relatively low values of $SEDD(\mathbf{r})$ represent electrons localized in atomic shells, while its high values, the overlapping regions. Maxima of $SEDD(\mathbf{r})$ in the overlap region where identified as boundaries between neighbouring shells. We have shown that the number of such defined shells agrees with the periodic table. The integration of the density over these shells yields electron numbers relatively close to the ideal ones. Comparison with shell populations obtained from the Electron Localization Function indicates that SEDD performs better with respect to the average deviation, reducing it from 0.37 to 0.24 electron. Nevertheless, this is a somewhat arbitrary measure, therefore, we conclude that both

descriptors have comparable performance. The main advantage of SEDD over ELF is that it is based only on the density.

A modified definition of $SEDD(\mathbf{r})$ was introduced to restrict its values only to non-negative numbers. This was achieved by shifting the argument of the logarithmic transformation. Since this transformation was used only for the convenience of visualization, and the physical content lies in the quantity $\xi(\mathbf{r})$, such modification does not alter any important features of $SEDD(\mathbf{r})$ in representing bonding patterns.

This and previous works have shown that the picture provided by SEDD agrees qualitatively with intuition. This suggests that, although devised as a purely mathematical object, SEDD carries some physical information. The physical interpretation of $\xi(\mathbf{r})$, where $SEDD(\mathbf{r}) = \ln[1 + \xi(\mathbf{r})]$, is provided in terms of the gradient of the local kinetic energy and the volume of the Fermi sphere. This makes a link between SEDD and the theory of local representation of operators as well as brings in indirectly the reference system of the homogeneous electron gas.

Finally, we should stress that the introduction of SEDD in Ref. 21 follows the opposite path compared to the one followed in the literature, where the electron localization is frequently the starting point. In our original work, we started with a simple mathematical feature (single-exponential decay of density) and found that an arbitrarily chosen criterion designed to reveal it, reveals also highly intuitive chemical concepts. This includes bonding and aromaticity (shown in previous works) as well as the resolution of electron shells in atoms, as shown in the present work. Equation (9) shows that SEDD is not only a tool to detect a particular geometrical feature of electron density but can also be seen as a tool to visualize a physical property. In contrast to ELF, which provides a direct measure of localization, SEDD relates to local deviations of a well-defined physical quantity in the analysed density (gradient of a local wave vector representation of the kinetic energy operator) from the volume of the Fermi sphere in the same-density homogeneous electron gas. Both quantities serve as measures of the number of overlapping one-electron states in their respective systems.

ACKNOWLEDGMENTS

This work was supported by the International Ph.D.-studies program at the Faculty of Chemistry Jagiellonian University within the Foundation for Polish Science MPD Program co-financed by the European Union (EU) European Regional Development Fund and the Grant from Swiss National Science Foundation (NSF(CH)) (200020/134791/1 FNRS).

[1] J. Waber and D. T. Cromer, J. Chem. Phys. **42**, 4116 (1965).
[2] P. Politzer and R. G. Parr, J. Chem. Phys. **64**(11), 4634–4637 (1976).
[3] R. J. Boyd, J. Chem. Phys. **66**, 356–358 (1977).
[4] A. M. Simas, R. P. Sagar, A. C. Ku, and V. H. Smith, Jr., Can. J. Chem. **66**(8), 1923–1930 (1988).
[5] R. F. Bader, *Atoms in Molecules: A Quantum Theory* (Oxford University Press, 1994).
[6] Z. Shi and R. J. Boyd, J. Chem. Phys. **88**, 4375 (1988).
[7] J. M. del Campo, J. L. Gázquez, R. J. Alvarez-Mendez, and A. Vela, Int. J. Quantum Chem. **112**(22), 3594–3598 (2012).
[8] M. Kohout, Int. J. Quantum Chem. **83**(6), 324–331 (2001).
[9] K. Wagner and M. Kohout, Theor. Chem. Acc. **128**(1), 39–46 (2011).
[10] M. Kohout, A. Savin, and H. Preuss, J. Chem. Phys. **95**(3), 1928 (1991).
[11] A. Nagy and N. March, Mol. Phys. **90**(2), 271–276 (1997).
[12] H. J. Bohórquez and R. J. Boyd, J. Chem. Phys. **129**, 024110 (2008).
[13] J. Tao, G. Vignale, and I. Tokatly, Phys. Rev. Lett. **100**(20), 206405 (2008).
[14] K. Finzel and M. Kohout, Theor. Chem. Acc. **132**(11), 1392 (2013).
[15] A. D. Becke and K. E. Edgecombe, J. Chem. Phys. **92**, 5397 (1990).
[16] M. Kohout and A. Savin, Int. J. Quantum Chem. **60**(4), 875–882 (1996).
[17] L. Bartell and L. Brockway, Phys. Rev. **90**(5), 833 (1953).
[18] R. J. Boyd, J. Phys. B **9**(5), L69 (1976).
[19] H. Weinstein, P. Politzer, and S. Srebrenik, Theor. Chim. Acta **38**(2), 159–163 (1975).
[20] P. W. Ayers and R. G. Parr, Int. J. Quantum Chem. **95**(6), 877–881 (2003).
[21] P. de Silva, J. Korchowiec, and T. A. Wesolowski, ChemPhysChem **13**(15), 3462–3465 (2012).
[22] P. de Silva, J. Korchowiec, N. J. S. Ram, and T. A. Wesolowski, Chimia **67**(4), 253–256 (2013).
[23] T. Kato, Commun. Pure Appl. Math. **10**(2), 151–177 (1957).
[24] M. M. Morrell, R. G. Parr, and M. Levy, J. Chem. Phys. **62**, 549 (1975).
[25] S. Luo, Int. J. Theor. Phys. **41**(9), 1713–1731 (2002).
[26] H. J. Bohórquez and R. J. Boyd, Theor. Chem. Acc. **127**(4), 393–400 (2010).
[27] H. J. Bohórquez, C. F. Matta, and R. J. Boyd, Int. J. Quantum Chem. **110**(13), 2418–2425 (2010).
[28] W.-P. Wang and R. G. Parr, Phys. Rev. A **16**(3), 891 (1977).
[29] A. Zupan, J. P. Perdew, K. Burke, and M. Causa, Int. J. Quantum Chem. **61**(5), 835–845 (1997).
[30] E. R. Johnson, S. Keinan, P. Mori-Sanchez, J. Contreras-García, A. J. Cohen, and W. Yang, J. Am. Chem. Soc. **132**(18), 6498–6506 (2010).
[31] G. Te Velde, F. M. Bickelhaupt, E. J. Baerends, C. Fonseca Guerra, S. J. van Gisbergen, J. G. Snijders, and T. Ziegler, J. Comput. Chem. **22**(9), 931–967 (2001).
[32] M. Kohout, DGrid, version 4.6, Radebeul, 2011.